heritage

MDPI

Article

Hidden Patterns in Pottery Fabrics: X-Ray μCT-Based 3D Pore Orientation Analysis to Differentiate Wheel-Throwing and Wheel-Coiling Ceramic Forming Techniques in Whole Vessels

Ilaria Caloi [1,*], Federico Bernardini [1,2,*] and Marco Voltolini [3]

[1] Dipartimento di Studi Umanistici, Università Ca' Foscari Venezia, 30123 Venice, Italy
[2] Multidisciplinary Laboratory, Abdus Salam International Center for Theoretical Physics, 34151 Trieste, Italy
[3] Dipartimento di Scienze della Terra "Ardito Desio", Università degli Studi di Milano, 20122 Milano, Italy; marco.voltolini@unimi.it
* Correspondence: icaloi@unive.it (I.C.); federico.bernardini@unive.it (F.B.)

Abstract

Identifying primary ceramic forming techniques is often problematic when surface traces are altered or erased by secondary shaping on the potter's wheel, particularly in vessels combining hand-building and wheel use. This study aims to develop a quantitative, non-destructive method to distinguish wheel-throwing and wheel-coiling techniques by analyzing internal fabric features. Experimental replicas of Middle Minoan handleless conical cups (18th cent. BC), produced using wheel-throwing-off-the-hump and wheel-coiling techniques, were investigated using X-ray micro-computed tomography (μCT). Macropores were segmented from complete 3D μCT datasets and their shape preferred orientation was quantitatively assessed through ellipsoid fitting, orientation distribution functions, and pole figure analysis. The results reveal systematic and reproducible differences between the two forming techniques: wheel-coiled vessels show predominantly horizontal pore elongation, expressed as equatorial girdle textures and vertically clustered short axes, whereas wheel-thrown vessels display inclined pore orientations, forming displaced girdles and ring-like short-axis distributions. These contrasting orientation patterns reflect distinct deformation fields imposed during vessel shaping. The study demonstrates that quantitative 3D analysis of pore orientation in whole vessels provides reliable criteria for identifying ceramic forming techniques and confirms previous qualitative observations. This approach offers a robust framework for technological analysis of ceramics and can be applied to both complete vessels and suitably oriented fragments.

Keywords: X-ray μCT; experimental archaeology; wheel-throwing; wheel-coiling; pore orientation quantification; ceramic forming technique identification

Academic Editor: João Pedro Veiga

Received: 18 March 2026
Revised: 15 April 2026
Accepted: 17 April 2026
Published: 22 April 2026

1. Introduction

The potter's wheel has been employed in antiquity through diverse operational modes. In certain manufacturing traditions, vessels were exclusively shaped on the wheel, engaging rotational kinetic energy (RKE) from the outset of production [1–3]. This practice encompasses techniques such as wheel-throwing and throwing-off-the-hump. In contrast, other traditions incorporated the potter's wheel solely during a second stage of the manufacturing process, when the vessel's rough-out had already been built through hand-building [2].

Documentation of forming techniques that integrate hand-building with the use of the potter's wheel is extensive, particularly in regions such as the Southern Levant [2], Mesopotamia [4], and the Aegean [5–7]. Here, the preference for coil-building combined with wheel rotation (referred to as wheel-coiling) predominates, although alternative hand-building methods are also noted [8–10]. For Minoan Crete, recent studies have shown that in northern and eastern Crete, after the first adoption of the potter's wheel in Middle Minoan IB (circa 1900 BC), corresponding to the beginning of the Protopalatial period, the wheel-coiling technique was the most common forming technique across the whole Middle Bronze Age [5,7], with only some classes of vessels (mainly plain handleless conical cups) also produced entirely on the potter's wheel [11,12]. In contrast, in southern Crete, and especially at Phaistos, different forming techniques co-existed in the Middle Bronze Age: most vessels are made in a combination of hand-building and the wheel (e.g., wheel-pinching and wheel-layering), some classes of vases are produced through the wheel-throwing techniques, and some vessels, especially in crude ware, are entirely handmade [8–10,13].

For the study of wheel-made vases, whether produced directly on the potter's wheel (i.e., wheel-thrown) or with the help of the potter's wheel (i.e., wheel-shaped or wheel-fashioned), the main concern is to understand the primary forming technique adopted. Macroscopic analysis alone is often not sufficient to identify the primary forming techniques used to produce a vessel, especially if there is a combination of hand-building and potter's wheel use. The latter can indeed obliterate the surface traces imparted by the primary forming technique [1,3,14].

Recent studies have developed new methods to investigate primary forming techniques. In comparison with the traditional 2D X-ray radiography [15,16], the X-ray μCT, with its complex imaging approach, has greatly facilitated a deeper 3D understanding of archaeological materials. In the last 15 years, several studies have demonstrated the ability of X-ray μCT scanning for the identification of macrostructural features (e.g., joins and other discontinuities) on hand-made vases [17–21] and most recently on wheel-made vases as well [22–24]. Furthermore, μCT analysis has seen greater application to examining the preferential orientation of particles and voids within pottery fabrics [19,25–27]. In particular, a recent study conducted on experimental vases reproducing Minoan cups [23] has shown that the combination of traditional macroscopic analysis with μCT-derived data—specifically the identification of joints through virtual sectioning, the visualization of topographic thickness variation in pottery walls, and the orientation of voids—is able to reveal differences between wheel-made vases produced entirely on the potter's wheel (i.e., wheel-thrown) and those combining hand-building and the device's use (e.g., wheel-coiled and wheel-pinched). For example, cups produced through the throwing-off-the hump technique [23] (Group 1) feature a measurable thickness that diminishes from the base of the walls up to the rim, and show a distinct void orientation: in the frontal view (i.e., from the side) voids have a diagonal orientation, originating almost from the bottom of the cups; when viewed perpendicularly to the bottom of the cups, these voids form a spiral pattern [23]. Differently, cups modeled using the wheel-coiling technique exhibit horizontal lines and/or fissures that are macroscopically visible and an irregular thickness topography [23] (Group 4). Technological joints can be detected in virtual sections and, in some cases, bands derived from the original coils still create thickness anomalies [23]. Concerning void orientation, voids retain the primary horizontal orientation imparted by the coils and, when observing the vessel bases perpendicularly, a clearly discernible concentric arrangement of voids is evident [23].

However, the evaluation of void orientation in complete vessels has so far been limited to qualitative analyses of μCT data [23]. A quantitative approach able to test these preliminary results and provide a parameter-based 3D method for investigating pottery-forming techniques in whole vessels is still lacking. Until now, quantitative analyses of μCT-derived data have only been applied to small samples (e.g., [28]), not to whole vases. Recent applications of small-angle neutron scattering (SANS) have yielded significant results in identifying pottery-forming techniques [29], yet these remain based on the separate analysis of portions of the ceramic body.

This study introduces, for the first time, a 3D quantitative method for identifying pottery-forming techniques through the analysis of void orientation in complete μCT datasets.

2. Materials and Methods

2.1. Materials: The Use of Experimental Replicas of Minoan Cups

The materials used for this study are experimental replicas of wheel-made Bronze Age (Minoan) cups typical of Crete. The type is a plain handleless conical cup, locally produced in the Minoan site of Phaistos (Crete) during the M(iddle) M(inoan) IIA period, corresponding to the 18th cent. BC [13]. It is short (h. 4.5–5.5 cm), with a conical profile on a very small and raised base (diam. 2.5–3.2 cm). This cup is much attested at Phaistos and is manufactured using different forming techniques, ranging from wheel-throwing techniques (i.e., throwing-off-the-hump and from a solid clay ball) to a combination of hand-building techniques with the use of the potter's wheel (e.g., wheel-coiling and wheel-pinching).

The replicas were produced by the Cretan potter V. Politakis in collaboration with I. Caloi. The experimental work was undertaken using materials and tools employed in Minoan times, revealed through the archaeological evidence from Minoan palatial Crete. First of all, the natural clays used were collected from southern Crete, and specifically Moni Odighitria and Vori, which are close to Phaistos. The clay sources are compatible with those used in the Early and Middle Bronze Ages to produce fine decorated pottery [30], and especially the Fine Painted Ware dating to Early Minoan II and the well-known polychrome Kamares Ware of the Protopalatial period [31]. Two different clays were mixed—one gray and one *terra rossa*—and no tempering was added, only water. This choice was made because most of the conical cups from the MM IIA deposits of Phaistos are produced in a very fine and pure fabric, which does not show inclusions, but the natural inclusions of the clay. For experimental reproductions a Minoan-type potter's wheel was adopted. It was constructed by the potter Vassilis Politakis on the basis of the models proposed by D. Evely for the broad Palatial period on Crete [32] (type 3C) [33] (p. 270) and by J. Morrison [34]. The clay discs used as wheel heads for the experiments are similar to the ones found at Protopalatial Malia [32,35] (pp. 111–112, pl. 50), [36] (p. 34). They were constructed by the potter V. Politakis with a diameter of 29–30 cm [13]. The potter's wheel was used with the help of an assistant, who rotated the axle, leaving the potter to work seated with both free hands. The speed used to shape and/or throw the experimental cups on the wheel was between 85 and 140 rpm [13]. The tools used for the experiments were made of bronze and bone. The tool adopted to apply water on the experimental vases was a natural sponge, while the strand used to cut the vases from the wheel surface was made of six hairs of a donkey tail. The vases were fired at 720–800 degrees in a pit-kiln reconstructed by Vassilis Politakis following the Minoan kilns identified at Phaistos and dating to the Pre- and Protopalatial period [37] (p. 153), [38].

A total amount of 60 replicas was manufactured. As explained in detail elsewhere [13,23], the experimental cups have been produced using the four following forming techniques: (1) throwing-off-the-hump technique (Group 1 with 25 replicas); (2) throwing from a solid

clay ball (Group 2 with 20 replicas); (3) wheel-pinching, that is, pinching and then shaping on the wheel (Group 3 with 10 replicas); (4) and wheel-coiling, i.e., a combination of coil-building using three coils of 1 cm each built on a circular base and shaping on the wheel (Group 4 with 15 replicas).

For this paper three replicas from Group 1 (replicas: H3, H14, H21; Figure 1d–f) and three from Group 4 were used (replicas: 3C2, 3C5, 5CW; Figure 1a–c). Experimental cups from Group 1 were produced using the throwing-off-the-hump technique, that is, fashioning small vases from the clay at the top of a large lump, also called a mound (Figure 2c,d). Placing the mound on the wheel as one piece, it was centered starting from the top; then the clay was pressed down against the wheel head as it was centered. The second step was opening up the very top of the mound and pulling the clay up to make the cup. Finally, the cup was cut off the hump with the strands of hair.

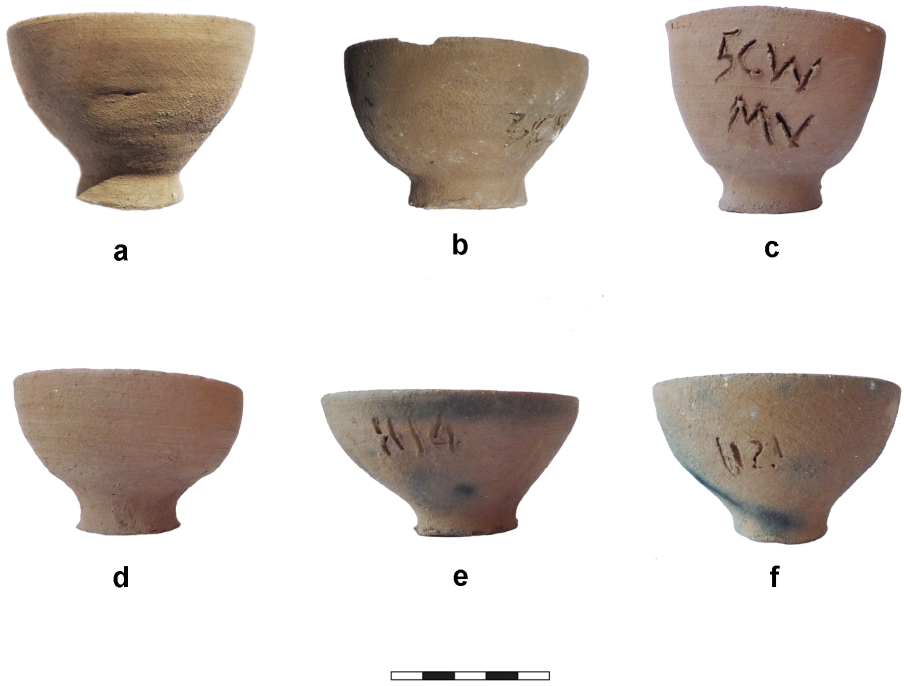

Figure 1. Replicas of Minoan cups produced using the wheel-coiling technique (**a**–**c**) and the wheel-throwing-off-the-hump technique (**d**–**f**). Scale bar: 5 cm.

Experimental cups from Group 4 were produced using wheel-coiling, i.e., a technique involving first the coil-building of a cup and then its final shaping on the wheel (Figure 2a,b). Three coils of 1 cm thickness were used and then set on a circular base 1 cm thick and 3 cm across. The joints between the coils were oriented towards the interior according to the traces of coils left on the archaeological cups from MM IIA deposits of Phaistos. Once the coils were positioned, the wheel was exploited for joining the coils, thinning the walls, and shaping the roughout; when the latter was achieved, the pot was finally shaped on the wheel. This technique corresponds to the wheel-coiling Method 3, first defined by V. Roux and Courty [2] and then recognized by C. Jeffra [7] in Minoan ceramics.

Figure 2. The two ceramic forming techniques used for the experimental work: wheel-coiling (**a**,**b**) and throwing off-the-hump (**c**,**d**).

2.2. X-Ray Micro-Computed Tomography

µCT analysis was conducted on six cups at the Multidisciplinary Laboratory (MLAB) of the Abdus Salam International Centre for Theoretical Physics. The system employed was purpose-built for archaeological and paleoanthropological investigations by the MLAB group, in collaboration with Elettra Sincrotrone Trieste. The system was designed to investigate relatively large objects, with lateral dimensions of up to about 20 cm and a maximum weight of around 15 kg. Under these conditions the system achieves voxel sizes of approximately 50–100 µm, while smaller samples can be analyzed at higher resolutions, reaching voxel sizes of about 5–10 µm [39].

This instrument complements other microtomography facilities already operating at Elettra. X-rays are generated by a Hamamatsu microfocus source (L8121–03) with a maximum voltage of 150 kV, a maximum current of 500 mA, and a minimum focal spot size of 5 µm. The detector consists of a Hamamatsu CMOS flat panel coupled to a fiber-optic plate beneath a GOS scintillator (C7942SK-25; 50 µm pixel size).

The source–detector system and the sample manipulation unit are mounted on a flexible mechanical structure that can be easily disassembled. The detector and motion system were selected from several available options to ensure both high precision and transportability. The overall configuration was conceived to create a mobile instrument that can be transported and installed in museums or other locations, enabling in situ analyses of valuable artefacts. At present, microCT experiments are carried out in the MLAB within a lead-shielded cabinet.

The system was also designed to allow relatively large sample-to-detector distances in order to exploit phase-contrast effects. Three-dimensional images are reconstructed from large series of two-dimensional radiographs—typically between about 1800 and 2500 projections—using dedicated mathematical reconstruction algorithms. This approach al-

lows the microstructure of materials to be examined at the micrometer scale through virtual sectioning and 3D rendering techniques. For data acquisition, commercially available software has been adapted and implemented.

Acquisition parameters were set to 110 kV, 90 µA, and 2 s exposure per projection, with 1440 projections taken over a full 360° rotation. The beam was filtered through a 0.01 mm copper plate. Data were reconstructed in 32-bit format using DigiXCT software (Digisens), yielding isotropic voxels of 40 µm.

2.3. Quantitative Characterization of Pore Shape Preferred Orientation

The orientation of pores provides key insights into ceramic forming techniques, making quantitative characterization of their shape preferred orientation (SPO) essential. In the study by Gait et al. [28], both morphometric parameters and an Orientation Index of macropores in vase fragments were evaluated. Here, we focus exclusively on orientation and applying a more detailed SPO analysis. This more refined approach enables the detection of subtle textural features, providing clearer and more robust criteria for distinguishing between ceramic forming techniques. This X-ray µCT-based SPO analysis has been already applied across disciplines, for example, to quantify vesicle alignment in deformed volcanic rocks [40] and to compare the SPO of phyllosilicates in metamorphic rocks with crystallographic preferred orientations obtained from neutron diffraction [41]. Voids such as volcanic vesicles or macropores in ceramics and other engineered materials are ideal targets for SPO analysis using X-ray µCT datasets. For a detailed methodological overview, we refer the reader to Voltolini et al. [40]; here, the same software is employed, with updates and improvements, but keeping the core functionalities and approach.

The workflow consists of the following steps:

1. Preprocessing: Filtering of X-ray µCT volumes in ImageJ/Fiji 1.54p [42] with an edge-preserving bilateral filter to suppress noise.
2. Segmentation: Automated thresholding with the Otsu method [43] to isolate macropores; pores connected to the sample surface are excluded because they are not identified by the applied procedure.
3. Morphometric analysis: Segmented volumes are processed directly in Blob3D [44]. Since macropores are already isolated, separation is unnecessary, and automated morphometric analysis can be applied.
4. Orientation analysis: Results are exported to Matlab® 2022b scripts incorporating the MTEX toolbox [45] to compute orientation distribution functions (ODFs) and pole figures (PFs) for the three principal axes of ellipsoids fitted to the pores. A texture-by-number approach is adopted, where each pore contributes equally, ensuring robust statistical characterization of orientations (as opposed to texture-by-volume, which weights orientations by pore size).
5. Visualization: Orientation parameters, particularly the angles of pore elongation axes, are mapped onto volume renderings using color scales. In the case of vases, the key feature is the orientation of elongation axes relative to the wheel rotation axis: horizontally aligned pores will show misorientation values close to 90°, whereas vertically aligned pores approach 0°.

Combined, PFs and misorientation-labeled volume renderings provide a comprehensive description of SPO in the vases. PFs yield intuitive visualizations of sample texture, while color-labeled renderings highlight the contribution of individual pores. PFs are shown for both long axes (directions of maximum pore stretching) and short axes (directions of maximum compression). Since the forming techniques impose distinct deformation fields, the resulting SPO is expected to vary between vases, with specific textures and alignment patterns in the PFs reflecting the shaping methods used.

3. Results

X-ray μCT measurements provided digital 3D models of the replicas, enabling quantitative assessment of macropore SPO. Figure 3 shows two examples: one wheel-coiled from Group 4 (left) and one wheel-thrown from Group 1 (right).

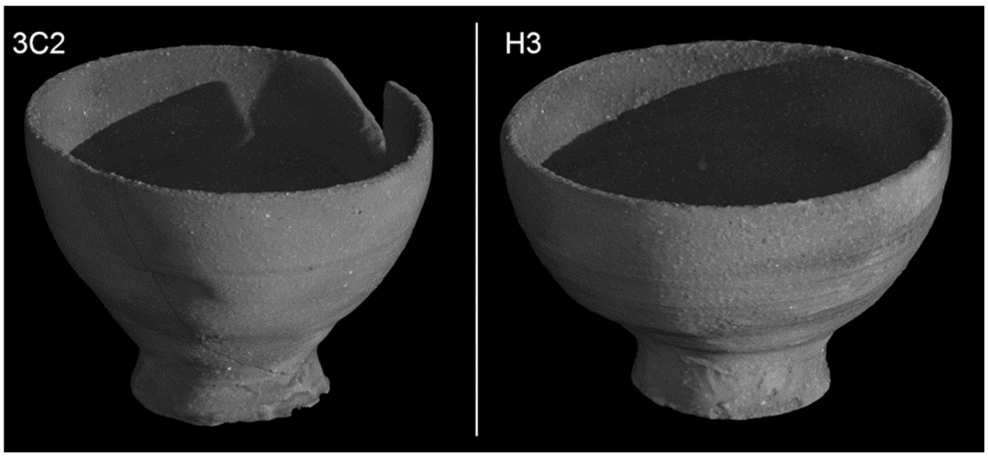

Figure 3. Volume rendering of the 3C2 and H3 cups, as measured via X-ray μCT.

To investigate pore textures, we quantified the SPO. As a first step, volume renderings were produced for six samples (Figure 4), including three wheel-coiled (left column) and three wheel-thrown (right column).

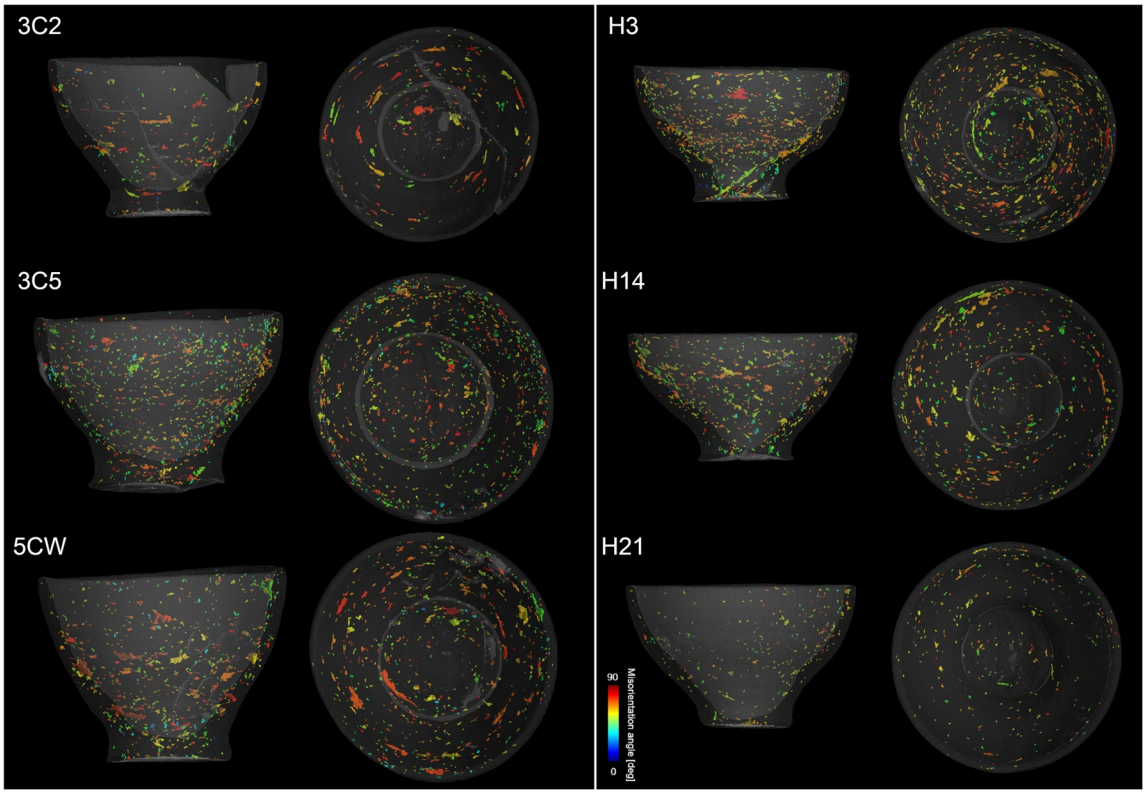

Figure 4. Volume renderings of six cups viewed from the side and top. The cup surfaces are shown as semi-transparent gray, and pores are colored according to misorientation of their long axis relative to the vertical symmetry axis.

The key features in Figure 4 are the pores, highlighted by rendering the solid material highly transparent gray. Each pore is colored according to its elongation-axis misorientation

with respect to the vertical axis: hot colors indicate nearly horizontal alignment, cold colors indicate vertical alignment, and intermediate colors (green/blue) represent ~45° orientations, as exemplified by the large basal pore in the H3 sample. This representation effectively captures local textures, but it is less suited for identifying global patterns. A preliminary comparison suggests more horizontal pores (hot colors) in wheel-coiled cups, but visual assessment alone is insufficient, and misorientation must be quantified. Misorientation values were therefore compiled into normalized histograms (Figure 5).

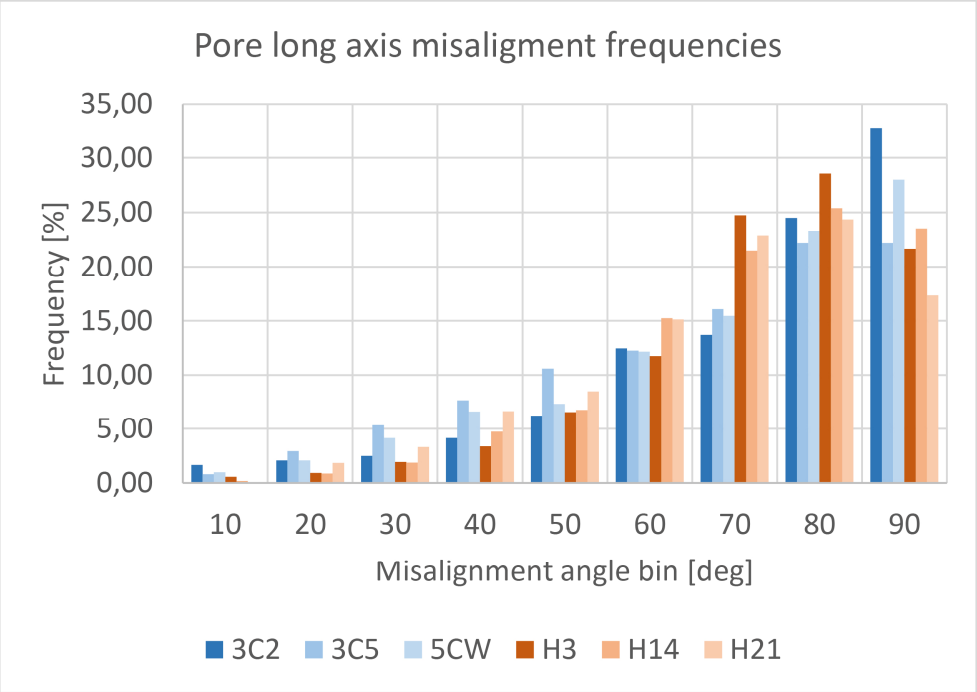

Figure 5. Normalized frequency histograms of the pore elongation direction misorientation values for the samples in Figure 3.

The histograms reveal systematic differences between replicas produced using the wheel-coiling and wheel-throwing techniques. Wheel-coiled samples show a higher proportion of pores with low misorientation, but the main feature is a peak in the 80–90° bin, indicating predominantly horizontal elongation. Wheel-thrown samples, in contrast, display their maxima in the 70–80° bin, suggesting elongation at an inclined angle rather than strictly horizontal. This distinction already highlights the imprint of forming techniques on pore SPO, but to capture the full textural pattern, orientation distribution functions (ODFs) and pole figures (PFs) were computed.

PFs (Figure 6) provide the clearest characterization of SPO and its relation to the ceramic forming technique. In wheel-coiled replicas (left column), the long axes form equatorial girdles, consistent with the histogram peak at 90°. Correspondingly, the short axes cluster near the PF center, reflecting vertical flattening. Sample 3C5 shows slightly less evident features due to vessel tilt (~15° SW), yet the equatorial-girdle pattern remains dominant.

In wheel-thrown replicas (right column), textures retain a cylindrical symmetry (in accordance with the forming technique) but differ markedly from wheel-coiled samples. Long axes still form girdles, but displaced from the equator—analogous to tropical latitudes on a globe—consistent with the histogram maxima at 70–80°. This produces paired rings in opposite hemispheres. Short axes also differ: instead of a central maximum, they tend to form annuli near the PF center, especially evident in H3.

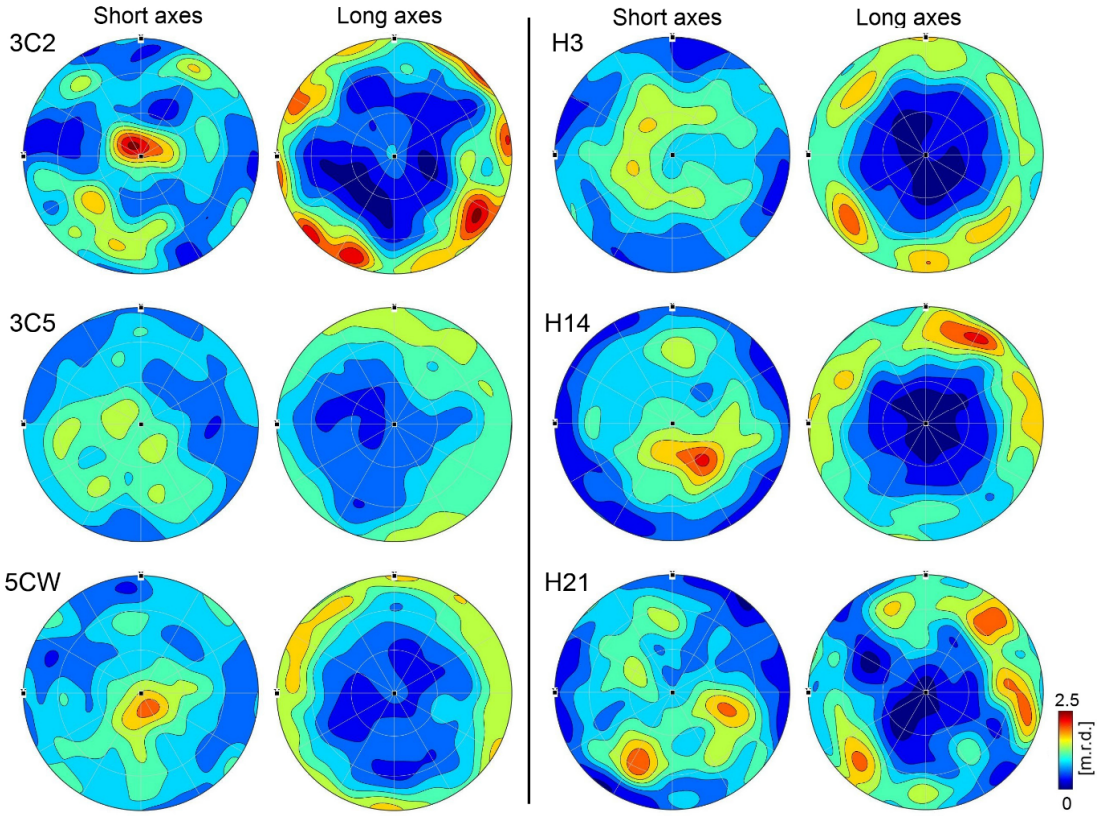

Figure 6. Pole figures relative to the long and short axes of the pores, in the six cups. Values are plotted in multiples of random distribution [m.r.d.], equal area projection, and upper hemisphere.

Together, these results demonstrate that manufacturing techniques impart distinct SPO signatures. Wheel-coiled replicas exhibit horizontally elongated and vertically flattened pores, resulting in sharper maxima in the center of the PFs, while wheel-thrown replicas develop inclined elongations and ring-like short-axis distributions. PF analysis thus provides a robust means to distinguish forming techniques in ceramic vessels.

4. Discussion and Conclusions

The SPO analysis presented here provides a comprehensive characterization of μCT-derived data from whole ceramic vessels. Examining complete vessels was crucial, primarily from a validation perspective, but also because different forming techniques were sometimes employed to produce distinct portions of the same vessel (e.g., [46]). The results are therefore both representative and reliable.

From an applied standpoint, however, the findings enable broader generalization. As long as the vessel's symmetry axis can be established—based, for instance, on the base or part of the rim—the SPO of the pores can be measured to determine whether the texture corresponds to an equatorial girdle (indicative of coiling) or to a ring-like distribution (indicative of wheel-throwing). Even in the case of fragments, partial fabrics would reproduce a subset of the patterns presented here, still providing sufficient information to identify the forming technique.

This study confirms the qualitative results obtained by Caloi and Bernardini [23] and successfully introduces a three-dimensional quantitative approach for identifying pottery-forming techniques based on a detailed SPO analysis in μCT datasets of whole vessels.

Author Contributions: I.C.: Conceptualization, methodology, project administration, writing—original draft preparation, writing—review and editing, funding acquisition. F.B.: Conceptualiza-

tion, methodology, software, visualization, writing—original draft preparation, writing—review and editing, funding acquisition. M.V.: Conceptualization, methodology, software, writing—original draft preparation, writing—review and editing. I.C. authored Sections 1 and 2.1, F.B. authored Sections 1 and 2.2, M.V. authored Section 2.3. The authors co-authored Sections 3 and 4. All authors have read and agreed to the published version of the manuscript.

Funding: This research was funded by the Ca' Foscari University of Venice.

Data Availability Statement: μCT data are available at https://zenodo.org/records/12743544.

Conflicts of Interest: The authors declare no conflicts of interest.

References

1. Courty, M.-A.; Roux, V. Identification of wheel-throwing on the basis of ceramic surface features and microfabrics. *J. Archaeol. Sci.* **1995**, *22*, 17–50. [CrossRef]
2. Roux, V.; Courty, M.-A. Identification of wheel-fashioning methods: Technological analysis of 4th–3rd millennium BC Oriental ceramics. *J. Archaeol. Sci.* **1998**, *25*, 747–763. [CrossRef]
3. Roux, V. *Ceramics and Society: A Technological Approach to Archaeological Assemblages*; Springer: Cham, Switzerland, 2019.
4. Baldi, S.; Roux, V. The innovation of potter's wheel: A comparative perspective between Mesopotamia and the southern Levant. *Levant* **2016**, *46*, 236–253. [CrossRef]
5. Knappett, C. Tradition and innovation in pottery forming technology: Wheel-throwing at Middle Minoan Knossos. *Annu. Br. Sch. Athens* **1999**, *94*, 101–129. [CrossRef]
6. Choleva, M. The first wheelmade pottery at Lerna: Wheel-thrown or wheel-fashioned? *Hesperia* **2012**, *81*, 343–381. [CrossRef]
7. Jeffra, C. A reexamination of early wheel potting in Crete. *Annu. Br. Sch. Athens* **2013**, *108*, 31–49. [CrossRef]
8. Todaro, S. Shaping tools and finished products from a pottery production area at Phaistos: A combined approach to the study of forming techniques in Early and Middle Minoan Crete. *Creta Antica* **2016**, *17*, 273–325.
9. Todaro, S. What is essential is invisible to the eye. Multi-layered and internally supported vases at Protopalatial Phaistos. In *Rhadamanthys. Studi di Archeologia Minoica in Onore di Filippo Carinci per il suo 70° Compleanno (BAR IS 2884)*; Baldacci, G., Caloi, I., Eds.; Oxford University Press: Oxford, UK, 2018; pp. 39–48.
10. Caloi, I. Identifying wheel-thrown vases in Middle Minoan Crete? Preliminary analysis of experimental replicas of plain handleless conical cups from Protopalatial Phaistos. *Intediscip. Archaeol.* **2021**, *XII*, 201–216. [CrossRef]
11. MacGillivray, J.A. *Knossos: Pottery Groups of the Old Palace Period*; BSA Studies 5; The British School at Athens: London, UK, 1998.
12. Berg, I. X-radiography of Knossian Bronze Age vessels: Assessing our knowledge of primary forming techniques. *Annu. Br. Sch. Athens* **2009**, *104*, 137–173. [CrossRef]
13. Caloi, I. Breaking with tradition? The adoption of the wheel-throwing technique at Protopalatial Phaistos: Combining macroscopic analysis, experimental archaeology and contextual information. *ASAtene* **2019**, *97*, 9–25.
14. Van der Leeuw, S.E. *Studies in the Technology of Ancient Pottery*; University of Amsterdam: Amsterdam, The Netherlands, 1976.
15. Rye, O.S. Pottery manufacturing techniques: X-ray studies. *Archaeometry* **1977**, *19*, 205–211.
16. Berg, I.; Ambers, J. X-Radiography of Archaeological Ceramics. In *The Oxford Handbook of Archaeological Ceramic Analysis*; Hunt, A.M.W., Ed.; Oxford University Press: Oxford, UK, 2017; pp. 101–114.
17. Bernardini, F.; Leghissa, E.; Prokop, D.; Velušcek, A.; De Min, A.; Dreossi, D.; Donato, S.; Tuniz, C.; Princivalle, F.; Montagnari Kokelj, M. X-ray computed microtomography of Late Copper Age decorated bowls with cross-shaped foots from central Slovenia and the Trieste Karst (North-Eastern Italy): Technology and paste characterisation. *Archaeol. Anthropol. Sci.* **2019**, *11*, 4711–4728. [CrossRef]
18. Bernardini, F.; Tuniz, C.; Zanini, F. X-ray computed microtomography for paleoanthropology, archaeology, and cultural heritage. In *Advanced Nanomaterials, Nanotechnologies and Nanomaterials for Diagnostic, Conservation and Restoration of Cultural Heritage*; Lazzara, G., Fakhrullin, R., Eds.; Elsevier: Amsterdam, The Netherlands, 2019; pp. 25–45.
19. Kahl, W.A.; Ramminger, B. Non-destructive fabric analysis of prehistoric pottery using high-resolution X-ray microtomography: A pilot study on the late Mesolithic to Neolithic site Hamburg-Boberg. *J. Archaeol. Sci.* **2012**, *39*, 2206–2219. [CrossRef]
20. Kozatsas, J.; Kotsakis, K.; Sagris, D.; David, K. Inside out: Assessing pottery forming techniques with micro-CT scanning. An example from Middle Neolithic Thessaly. *J. Archaeol. Sci.* **2018**, *100*, 102–119. [CrossRef]
21. Thér, R. Ceramic technology. How to reconstruct and describe pottery-forming practices. *Archaeol. Anthropol. Sci.* **2020**, *12*, 172. [CrossRef]
22. Takenouchi, K.; Yamahana, K. Fine pottery shaping techniques in Predynastic Egypt: A pilot study on non-destructive analysis using an X-ray CT scanning system. *J. Archaeol. Sci. Rep.* **2021**, *37*, 102989. [CrossRef]

23. Caloi, I.; Bernardini, F. Revealing primary forming techniques in wheel-made ceramics with X-ray microCT. *J. Archaeol. Sci.* **2024**, *169*, 106025. [CrossRef]
24. Thér, R.; Mangel, T. Introduction of the potter's wheel as a reflection of social and economic changes during the La Tène period in Central Europe. *Archaeol. Anthropol. Sci.* **2024**, *16*, 1. [CrossRef]
25. Park, K.S.; Milke, R.; Rybacki, E.; Reinhold, S. Application of image analysis for the identification of prehistoric ceramic production technologies in the North Caucasus (Russia, Bronze/Iron Age). *Heritage* **2019**, *2*, 2327–2342. [CrossRef]
26. Sanger, M.; Thostenson, J.; Hill, M.; Cain, H. Fibrous twists and turns: Early ceramic technology revealed through computed tomography. *Appl. Phys. A Mater. Sci. Process.* **2013**, *111*, 829–839. [CrossRef]
27. Sanger, M.C. Investigating pottery vessel manufacturing techniques using radiographic imaging and computed tomography: Studies from the Late Archaic American Southeast. *J. Archaeol. Sci. Rep.* **2016**, *9*, 586–598. [CrossRef]
28. Gait, J.; Bajnok, K.; Szilágyi, V.; Szenti, I.; Kukovecz, Á.; Kis, Z. Quantitative 3D orientation analysis of particles and voids to differentiate hand-built pottery forming techniques using X-ray microtomography and neutron tomography. *Archaeol. Anthropol. Sci.* **2022**, *14*, 223. [CrossRef]
29. Gait, J.; Bajnok, K.; Hugot, N.; Horváth, F.; Pépy, G.; Ellis, D.; Len, A. Novel application of SANS provides quantitative non-destructive identification of forming techniques in late Roman and early medieval pottery from Pannonia. *Sci. Rep.* **2024**, *14*, 25926. [CrossRef] [PubMed]
30. Mentesana, R.; Amato, V.; Day, P.M.; Ghilardi, M.; Kilikoglou, V.; Longo, F.; Todaro, S. Looking for the invisible: Landscape change and ceramic manufacture during the Final Neolithic–Early Bronze Age at Phaistos. In *Géoarchéologie des Îles de Méditerranée*; Ghilardi, M., Ed.; CNRS Editions: Paris, France, 2016; pp. 299–310.
31. Day, P.M.; Relaki, M.; Faber, E.W. Pottery making and social reproduction in the Bronze Age Mesara. In *Pottery and Society: The Impact of Recent Studies in Minoan Pottery*; Wiener, M., Warner, J.L., Polonsky, J., Hayes, E., Eds.; Archaeological Inst of Amer: Boston, MA, USA, 2006; pp. 22–72.
32. Evely, R.D.G. The potter's wheel in Minoan Crete. *Annu. Br. Sch. Athens* **1988**, *83*, 83–126. [CrossRef]
33. Evely, R.D.G. *Minoan Crafts: Tools and Techniques. An Introduction*; SIMA 92.2; Paul Åströms Förlag: Jonsered, Sweden, 2000.
34. Evely, R.D.G.; Morrison, J.E. The Minoan potter's wheel: A study in experimental archaeology. In *Proceedings of the 6th International Congress on the Archaeology of the Ancient Near East*; Matthiae, P., Pinnock, F., Nigro, L., Marchetti, N., Eds.; Otto Harrassowitz: Wiesbaden, Germany, 2010; Volume I, pp. 283–288.
35. Poursat, J.-C. *Fouilles Exécutées à Malia: Le Quartier Mu III. Artisans Minoens: Les Maisons-Ateliers du Quartier Mu*; Études Crétoises XXXII; École française d'Athènes: Athènes, Greece, 1996.
36. Poursat, J.-C.; Knappett, C. *Fouilles Exécutées à Malia: Le Quartier Mu IV. La Poterie du Minoen Moyen II: Production et Utilisation*; Études Crétoises XXXIII; École française d'Athènes: Athens, Greece, 2005.
37. Todaro, S. *The Phaistos Hills Before the Palace: A Contextual Reappraisal*; Polimetrica: Monza, Italy, 2013.
38. La Rosa, V. Le campagne di scavo 2000–2002 a Festòs. *ASAtene* **2000**, *80*, 635–745.
39. Tuniz, C.; Bernardini, F.; Cicuttin, A.; Crespo, M.L.; Dreossi, D.; Gianoncelli, A.; Mancini, L.; Mendoza Cuevas, A.; Sodini, N.; Tromba, G.; et al. The ICTP-Elettra X-ray laboratory for cultural heritage and archaeology. *Nucl. Instrum. Methods Phys. Res. Sect. A* **2013**, *711*, 106–110. [CrossRef]
40. Voltolini, M.; Zandomeneghi, D.; Mancini, L.; Polacci, M. Texture analysis of volcanic rock samples: Quantitative study of crystals and vesicles shape preferred orientation from X-ray microtomography data. *J. Volcanol. Geotherm. Res.* **2011**, *202*, 83–95. [CrossRef]
41. Zucali, M.; Voltolini, M.; Ouladdiaf, B.; Mancini, L.; Chateigner, D. The 3D quantitative lattice and shape preferred orientation of a mylonitised metagranite from Monte Rosa (Western Alps): Combining neutron diffraction texture analysis and synchrotron X-ray microtomography. *J. Struct. Geol.* **2014**, *63*, 91–105. [CrossRef]
42. Schindelin, J.; Rueden, C.T.; Hiner, M.C.; Eliceiri, K.W. The ImageJ ecosystem: An open platform for biomedical image analysis. *Mol. Reprod. Dev.* **2015**, *82*, 518–529. [CrossRef]
43. Otsu, N. A threshold selection method from gray-level histograms. *Automatica* **1975**, *11*, 23–27. [CrossRef]
44. Ketcham, R.A. Computational methods for quantitative analysis of three-dimensional features in geological specimens. *Geosphere* **2005**, *1*, 32–41. [CrossRef]
45. Bachmann, F.; Hielscher, R.; Schaeben, H. Texture analysis with MTEX—Free and open source software toolbox. *Solid State Phenom.* **2010**, *160*, 63–68. [CrossRef]
46. Todaro, S. Forming techniques and cultural identity in Early and Middle Minoan Crete: Multi-layered vessels from a pottery production area at Phaistos. *ASAtene* **2017**, *95*, 127–141.